Virus-associated CD8+ T-cells are not activated through antigen-mediated interaction inside atherosclerotic lesions

Jong, M.J.M. de; Schaftenaar, F.H.; Depuydt, M.A.C.; Vigario, F.L.; Janssen, G.M.C.; Peeters, J.A.H.M.; ... ; Sluetter, B.

Arteriosclerosis, Thrombosis, and Vascular Biology

BASIC SCIENCES

Virus-Associated CD8+ T-Cells Are Not Activated Through Antigen-Mediated Interaction Inside Atherosclerotic Lesions

Maaike J.M. de Jong, Frank H. Schaftenaar, Marie A.C. Depuydt, Fernando Lozano Vigario, George M.C. Janssen, Judith A.H.M. Peeters, Lauren Goncalves, Anouk Wezel, Harm J. Smeets, Johan Kuiper, Ilze Bot, Peter van Veelen, Bram Slütter

INTRODUCTION: Viral infections have been associated with the progression of atherosclerosis and CD8+ T-cells directed against common viruses, such as influenza, Epstein-Barr virus, and cytomegalovirus, have been detected inside human atherosclerotic lesions. These virus-specific CD8+ T-cells have been hypothesized to contribute to the development of atherosclerosis; however, whether they affect disease progression directly remains unclear. In this study, we aimed to characterize the activation status of virus-specific CD8+ T-cells in the atherosclerotic lesion.

METHODS: The presence, clonality, tissue enrichment, and phenotype of virus-associated CD8+ T-cells in atherosclerotic lesions were assessed by exploiting bulk T-cell receptor-β sequencing and single-cell T-cell receptor (α and β) sequencing datasets on human endarterectomy samples and patient-matched blood samples. To investigate if virus-specific CD8+ T-cells can be activated through T-cell receptor stimulation in the atherosclerotic lesion, the immunopeptidome of human plaques was determined.

RESULTS: Virus-associated CD8+ T-cells accumulated more in the atherosclerotic lesion (mean=2.0%), compared with patient-matched blood samples (mean=1.4%; *P*=0.05), and were more clonally expanded and tissue enriched in the atherosclerotic lesion in comparison with nonassociated CD8+ T-cells from the lesion. Single-cell T-cell receptor sequencing and flow cytometry revealed that these virus-associated CD8+ T-cells were phenotypically highly similar to other CD8+ T-cells in the lesion and that both exhibited a more activated phenotype compared with circulating T-cells. Interestingly, virus-associated CD8+ T-cells are unlikely to be activated through antigen-specific interactions in the atherosclerotic lesion, as no virus-derived peptides were detected on HLA-I in the lesion.

CONCLUSIONS: This study suggests that virus-specific CD8+ T-cells are tissue enriched in atherosclerotic lesions; however, their potential contribution to inflammation may involve antigen-independent mechanisms.

GRAPHIC ABSTRACT: A graphic abstract is available for this article.

Key Words: antigen presentation ■ atherosclerosis ■ inflammation ■ peptide ■ viral infections

Atherosclerosis is a lipid-driven chronic inflammatory disease, which is characterized by the buildup of lipids and immune cells in the arterial wall, resulting in lesions that can partially occlude the vessel. Rupture of unstable lesions can result in atherothrombosis and lead to acute cardiovascular events such as myocardial infarction or stroke. Infectious diseases, like influenza virus A (IAV), Epstein-Barr virus (EBV), and cytomegalovirus, are independent risk factors for cardiovascular disease and a potential explanation for seasonal peeks of cardiovascular disease–related hospitalization that

See accompanying editorial on page 1315

Correspondence to: Bram Slütter, PhD, Division of BioTherapeutics, Leiden University, LACDR, Einsteinweg 55, 2333CC Leiden, the Netherlands. Email b.a.slutter@lacdr.leidenuniv.nl

Supplemental Material is available at https://www.ahajournals.org/doi/suppl/10.1161/ATVBAHA.123.320539.
For Sources of Funding and Disclosures, see page 1313.

Arterioscler Thromb Vasc Biol is available at www.ahajournals.org/journal/atvb

Nonstandard Abbreviations and Acronyms

AP-1	activation protein-1
COX	cytochrome c oxidase
EBV	Epstein-Barr virus
IAV	influenza A virus
MITRAC	Mitochondrial translation regulation assembly intermediate of cytochrome c oxidase
PMA	phorbol 12-myristate 13-acetate
TCRβ	T-cell receptor beta

Highlights

- Virus-associated CD8+ T-cells accumulate in atherosclerotic lesions and are more tissue enriched and clonally expanded compared with other CD8+ T-cells there.
- Virus-associated CD8+ T-cells are phenotypically highly similar to other CD8+ T-cells in the lesion.
- Virus-derived antigens are not being presented on HLA-I within atherosclerotic lesions of patients without a symptomatic virus infection.

coincide with the flu season.[1–4] The recent coronavirus disease 2019 (COVID-19) pandemic has emphasized this correlation between infection and cardiovascular disease, apparent from a significantly increased incidence of cardiovascular events after COVID hospitalization.[5] Moreover, vaccination against infectious diseases, like influenza, pneumococcal polysaccharide, and COVID-19 has been shown to reduce the incidence of cardiovascular events.[6–9]

The link between infectious diseases and the progression of atherosclerosis was first considered in the early 20th century.[10,11] Seventy years later, Fabricant et al[12] were the first to provide experimental evidence of the correlation between Marek disease virus, a chicken herpes virus, and atherosclerosis. Since then various infectious diseases have been associated with the progression of atherosclerosis, including respiratory pathogens (*Chlamydia pneumonia*, COVID-19, and influenza viruses),[13–15] gastric pathogens (*Helicobacter cinaedi, Helicobacter pylori*),[16,17] and herpes viruses (cytomegalovirus, EBV, and herpes simplex virus).[18–21]

Infectious diseases could affect the progression of atherosclerosis by directly infecting atherosclerotic tissue or indirectly, by inducing a systemic increase in proinflammatory mediators and immune cell numbers. Signs of direct infection of the human vasculature have been demonstrated for influenza, EBV, cytomegalovirus, and COVID-19 among others.[22–24] Moreover, CD8+ T-cells responsive against these infections have been detected inside human atherosclerotic lesions.[25,26] These virus-specific CD8+ T-cell responses in the atherosclerotic lesion may contribute to increased tissue damage and local secretion of proinflammatory mediators, including cytolytics, cytokines, and chemokines.

Recently, Chowdhury et al[26] demonstrated that about 3.5% of the CD8+ T-cells in human atherosclerotic lesions are associated with viral specificity. Part of these virus-associated CD8+ T-cells were clonally expanded in the lesion. Based on the clonal expansion of virus-associated CD8+ T-cells and the absence of viral infection, they implied that these virus-associated CD8+ T-cells might be cross-reactive to self-antigens.

Here, we aim to dissect whether virus-specific CD8+ T-cells are indeed activated in the atherosclerotic lesions and whether the activation depends on the recognition of pathogen-derived peptides, or self-peptides strongly mimicking pathogen-derived peptides (mimicry peptides) in the atherosclerotic lesion. We showed that virus-associated CD8+ T-cells are clonally expanded and tissue enriched in atherosclerotic lesions and have a more activated phenotype compared with virus-associated CD8+ T-cells in blood. Yet, virus-associated CD8+ T-cells are transcriptionally highly similar to other plaque-residing CD8+ T-cells. Finally, using an immunopeptidomics approach we demonstrate that virus-associated CD8+ T-cells are unlikely to be activated through antigen recognition in the atherosclerotic lesion and that if these CD8+ T-cells contribute to inflammation, they probably do so through mimicry or bystander activation.

MATERIALS AND METHODS

All scripts have been made publicly available on the GitHub and can be accessed at https://github.com/MaaikeJMdeJong/Virus-associated-CD8-T-cells-in-atherosclerosis. The mass spectrometry proteomics data have been deposited to the ProteomeXchange Consortium via the PRIDE[27] partner repository with the dataset identifier PXD049243.

Human Studies

Handling of all human samples complied with the Code for Proper Secondary Use of Human Tissue and are in accordance with the declaration of Helsinki regarding ethical principles for medical research involving human subjects and all patients signed an informed consent form.

For T-cell receptor beta (TCRβ) sequencing (samples from patients cohort 1) and the stimulation assay (samples from patients cohort 2), whole blood and atherosclerotic plaques samples were obtained from 10 patients who underwent carotid endarterectomy surgery at the Haaglanden Medical Center, Westeinde, The Hague, the Netherlands (study approval number cohort 1: Z19.075; protocol number: NL71516.058.19; study approval number cohort 2: 17-046; protocol number: NL57482.098.17). The immunopeptidome of the lesion was evaluated on endarterectomy samples of the carotid and femoral arteries of patients from cohort 1. Whole blood samples were collected before carotid endarterectomy via venipuncture.

Only atherosclerotic plaques from primary carotid endarterectomies were included in this study.

Whole Blood Processing and Plasma Isolation

Peripheral venous blood was collected in K2-ethylenediaminetetraacetic acid blood tubes (BD Vacutainer) and processed according to protocol described in study by Depuydt et al.[28] For cohort 1, whole blood samples were lysed twice in ACK (ammonium-chloride-potassium) lysis buffer for 10 minutes at room temperature, after which samples were washed with PBS (300*g*, 5 minutes). Cells were taken up in RPMI+1% fetal calf serum and stored in Cryostor cell cryopreservation medium (Sigma-Aldrich) at −80 °C until further use. For cohort 2, plasma was collected by spinning down whole blood samples at 250*g* for 5 minutes. Plasma was stored at −150 °C until further use. Next, peripheral blood mononuclear cells (PBMCs) were isolated using a Ficoll-Paque Premium (GE Healthcare) density gradient in SepMate PBMC isolation tubes (STEMCELL Technologies) following manufacturer's protocol. The intermediate layer containing PBMCs was isolated and washed twice with PBS+2% fetal calf serum (250*g*, 10 minutes, room temperature). Cells were stored in Cryostor cell cryopreservation medium (Sigma-Aldrich) at −150 °C until further use.

Human Atherosclerotic Plaque Cell Isolation

Human endarterectomy samples from cohort 1 and cohort 2 were digested into a single-cell suspension following the same protocol.[28] In brief, a section (1–5 mm) of the culprit segment of the lesion was stored at −80 °C for immunopeptidomics. The remainder of the lesion was digested into a single-cell suspension by cutting the tissue into pieces of ≈1 mm^2, followed by digestion with 2.5 mg/mL collagenase IV (Thermo Fisher Scientific), 0.25 mg/mL DNAse I (Sigma), 2.5 mg/mL human albumin fraction V (MP Biomedicals) in RPMI 1640 for 30 minutes at 37 °C. After digestion, plaque tissue was mashed over a 70-µm strainer to create a single-cell suspension and washed in RMPI 1640. Cells were cryostored in Cryostor cell cryopreservation medium (Sigma-Aldrich) at −80 °C until further use.

Bulk TCRβ Sequencing

Genomic DNA was isolated from single-cell plaque suspensions and patient-matched PBMC samples using a DNA extraction kit (Qiagen), following the manufacturer's protocol. VDJ sequences were curated using the Adaptive Biotechnology TCRβ sequencing platform.

Single-Cell TCR Sequencing

An in-house single-cell T-cell receptor (TCR) sequencing (scTCR-seq) data set was used to interrogate the phenotype of virus-associated CD8+ T-cells.[28] In brief, Depuydt et al performed scTCR-seq on whole blood and atherosclerotic lesions of 3 male patients who underwent carotid endarterectomy. PBMCs and single-cell plaque suspensions were stained with TotalSeq-C antibodies against CD3, CD4, CD8, and CD14. Plaque suspensions were also stained for CD45. ScTCR-seq was performed on PBMCs and live CD45+ plaque cells, using 10× Genomics 5′ Single Cell Immune Profiling technology. Next, CD8+ T-cells were subclustered from all T-cell clusters, based on their expression of CD8 (protein expression CD8>1.0), and absence of CD4 (protein expression CD4<0.75).

Selecting Virus-Specific CD8+ T-Cells

Virus-associated CD8+ T-cells were selected from human plaque bulk TCRβ sequencing and scTCR-seq data, by matching TCRα (only scTCR-seq data) or TCRβ sequences with public databases (VDJdb,[29] mcPAS,[30] and TBAdb[31]). These databases contain TCRβ sequences of known specificity, with information on the TCR sequence, the complementarity-determining region 3 sequence, the cognate epitope, and the origin of this epitope. From these public databases, all TCRβ sequences associated with infectious diseases were selected, excluding TCRs associated with noninfectious diseases, like cancer. These selected TCRβ sequences were matched with the TCRβ sequences from the human plaque obtained with bulk TCRβ sequencing or matched to the TCRα and TCRβ sequences curated during scTCR-seq using the tidyverse package in R-Script (Tables S1 and S2).[32] CD8+ T-cells that did not match one of the TCRβ sequences from the database are annotated as nonassociated.

To evaluate the proportion of virus-associated CD8+ T-cells at another site of chronic inflammation, a previously published dataset containing TCRβ sequencing data from synovial fluid and blood samples from psoriatic arthritis patients was utilized (data availability: ArrayExpress E-MTAB-11498).[33] Viral association of the TCRβ was determined as described above.

Phenotypic Characterization of Virus-Associated CD8+ T-Cells

Phenotypic differences between virus-associated CD8+ T-cells in plaque versus blood, and differences between plaque-residing virus-associated CD8+ T-cells relative to other CD8+ T-cells in plaque, were evaluated on scTCR-seq data using the FindMarkers function of Seurat, defining differential gene expression between groups by using a nonparametric Wilcoxon rank-sum test. Differentially expressed genes were visualized using EnhancedVolcano (Version 1.16.0).[34]

Clonal Expansion and Tissue-Enrichment Scores

T-cell clonality and tissue-enrichment scores were calculated as described previously.[28] In brief, CD8+ T-cell clonotypes were identified based on their TCRβ amino acid sequence. Clonotype frequency was determined per tissue per patient and was defined as the quantity of 1 specific TCRβ sequence in a tissue divided by a total number of TCRβ sequences within that tissue of the same patient. Patients with <5 virus-associated CD8+ T-cells in the lesion were excluded from the analysis, due to insufficient power. Based on the clonotype frequency, clonotypes were classified as hyperexpanded (clonotype abundance >10% and clonotype occurring more than once), large (clonotype abundance <10% and >1% and clonotype occurring more than once), medium (clonotype abundance <1% and >0.1% and clonotype occurring more than once), small (clonotype abundance <0.1% and clonotype occurring more than once), or single (clonotype occurring once). Moreover, the ratio between clonotype frequency in PBMC and plaque was used to determine the tissue-enrichment score. Based on the tissue-enrichment score, clonotypes were classified as plaque-enriched

([plaque clonotype %/PBMC clonotype %]>1.2 and clonotype occurring more than once in plaque), unenriched ([plaque clonotype %/PBMC clonotype %]=0.8–1.2, or clonotype occurring once in plaque and PBMC, or clonotype occurring once in tissue with the highest % of the clonotype), single (clonotype occurring once in plaque or PBMC), PBMC-enriched ([plaque clonotype %/PBMC clonotype %] <0.8 and clonotype occurring more than once in PBMC).

Cytomegalovirus Serology Measurement

To assess the prevalence of cytomegalovirus in our patients, cytomegalovirus serology was measured in the plasma of 20 patients from cohort 2. Cytomegalovirus serology was tested using the human anti-cytomegalovirus IgG ELISA Kit (cytomegalovirus; Abcam) according to manufacturer's protocol.

Stimulation Assay

To evaluate the cytokine production of virus-associated CD8+ T-cells in the lesion in response to external stimulation, 20 PM and plaque samples were stained with fluorescently labeled HLA-A2 restricted tetramers binding to influenza (GILGFVFTL) or EBV (GLCTLVAML)–specific T-cells in complete RPMI (RPMI 1640 [VWR] containing 10% FBS [Merck], 1% penicillin/streptomycin (Fisher Scientific) and 1% L-glutamine [VWR]) at 37 °C and 5% CO_2. Cells were subsequently stimulated for 4 hours with PMA (phorbol 12-myristate 13-acetate, 50 ng/mL, Sigma-Aldrich) and ionomycin (500 ng/mL, Sigma-Aldrich) in the presence of brefeldin A (Thermo Fisher Scientific) in complete RPMI at 37 °C and 5% CO_2. After stimulation, cells were extracellularly stained for 30 minutes at 4 °C (staining mix: Table S3). Before staining with the intracellular staining mix, cells were fixed and permeabilized using an intracellular staining kit (BD Bioscience) following the manufacturer's protocol. FACS measurements were performed on a Cytoflex S (Beckman and Coulter) and analyzed with FlowJo v10.7 (Treestar; San Carlos, CA). Tetramer gating was based on a fluorescence minus 1 control included for every patient. Only patients expressing a tetramer+ population (N=12) were included in further analysis. The applied gating strategy can be observed in Figure S1.

Immunoprecipitation

The immunopeptidome of human atherosclerotic lesions was determined by eluting peptides presented on HLA-I from 2.4 g of carotid and femoral endarterectomy samples, originating from a pool of 50 endarterectomy samples, as described previously.[35] Plaques were cut into small pieces, and lysis buffer was added (50 mmol/L Tris-Cl, pH 8.0, 150 mmol/L NaCl, 5 mmol/L ethylenediaminetetraacetic acid, 0.5% Zwittergent 3–12 [N-dodecyl-N,N-dimethyl-3-ammonio-1-propanesulfonate], and protease inhibitor [Complete, Roche Applied Science]), and the solution was probe sonicated on ice, followed by shaking for 2 hours at 0 °C. Lysates were centrifuged for 10 minutes at 2500*g* and for 45 minutes at 31 000*g* to remove nuclei and other insoluble material, respectively. Lysates were passed through a 50-µL CL-4B Sepharose column (in a standard yellow tip equipped with a filter) to preclear the lysate and subsequently passed through a 50-µL column containing 125-µg pan class I (W6/32) IgG (BioXcell) coupled to protein G Sepharose. The W6/32 column was subsequently washed with 250 µL of lysis buffer, 250 µL of low-salt buffer (20 mmol/L Tris-Cl; pH, 8.0; 120 mmol/L NaCl), 100 µL of high-salt buffer (20 mmol/L Tris-Cl; pH, 8.0; 1 M NaCl), and finally with 250 µL of the low-salt buffer. HLA-peptide complexes were eluted with 250 µL of 10% acetic acid, diluted with 1 mL of 0.1% trifluoroacetic acid, and purified by SPE (Oasis HLB, Waters) by sequential elution with 20%, 30%, and 40% acetonitrile in 0.1% trifluoroacetic acid to recover HLA peptides.

Mass Spectrometry

HLA peptides were analyzed by using an easy nLC1200 (Thermo, Bremen, Germany) coupled to an Orbitrap Fusion LUMOS mass spectrometer (Thermo). The injection was done onto a homemade precolumn (100 µm×15 mm; Reprosil-Pur C18-AQ 3 µm, Dr Maisch, Ammerbuch, Germany) and elution via a homemade analytical column (15 cm×50 µm; Reprosil-Pur C18-AQ 3 µm). The gradient was 0% to 30% solvent B (90% acetonitrile/0.1% trifluoroacetic acid) in 120 minutes. The analytical column was drawn to a tip of around 5 µm and acted as the electrospray needle of the mass spectrometry (MS) source.

The Orbitrap Fusion LUMOS mass spectrometer was operated in data-dependent MS/MS (top-N mode), with collision energy at 32 V and recording of the MS2 spectrum in the orbitrap. In the master scan (MS1), the resolution was 60 000, and the scan range 300 to 1400 at an AGC (automatic gain control) target of 400 000 at a maximum fill time of 50 ms. The dynamic exclusion was set after n=1 with an exclusion duration of 20 seconds. Charge states 1 to 4 were included. For MS2, precursors were isolated with the quadrupole with an isolation width of 1.2 Da. HCD (higher-energy collisional dissociation) collision energy was set to 32 V. First mass was set to 110 Da. The MS2 scan resolution was 30 000, with an AGC target of 50 000 at a maximum fill time of 100 ms. In a postanalysis process, Proteome Discoverer Version 2.1 was used for peptide and protein identification, using Mascot version 2.2.07 using a human database (20 596 entries) supplemented with a selection of viral and bacterial proteomes (Table S4). Oxidation (on methionine) and cysteinylation (on cysteine) were set as variable modifications. Precursor ion mass tolerance was set to 10 PM MS/MS fragment tolerance was 20 mmu. The false discovery rate was set at <1% and, in addition, peptides with mascot ion scores <35 were generally discarded. The immunopeptidomics analysis yielded 2304 HLA-I-derived peptides, listed in Table S5. Putative pathogen-derived peptides were manually assessed, followed by matching of the MS/MS spectrum of the eluted peptide and its synthetic counterpart (Table S6).

Mimicry Peptides

To identify molecular mimicry peptides, peptides presented on HLA-I were aligned with pathogenic proteomes, allowing for 1 mismatch in amino acid sequence (Table S7). To identify highly similar peptides, the approximate string matching function agrep was used in R-4.1.3.[36] Potential mimicry peptides are listed in Table S5. To predict if these molecular mimicry peptides could have been presented to the host immune system, the binding capacity of mimicry peptides with a length of 8 to 10 amino acids to a reference panel consisting of the 27 most frequently occurring HLA class I types in Europe was evaluated using the MHC-I (major histocompatibility complex) binding predictions tool of IEDB (http://tools.iedb.org/mhci/; Table S8).

Statistics

Data are presented in individual dot plots with bars indicating the mean and SD. Outliers were identified using a Grubbs outlier test (α=0.05), and the normality of the data was tested using a Shapiro-Wilk test. Data were analyzed using a 2-tailed ratio paired Student *t* test or a 2-tailed paired Student *t* test when comparing 2 groups, or a 2-way ANOVA with Bonferroni multiple comparisons test when comparing 2 groups with multiple conditions. Statistical analysis was performed using GraphPad Prism. Probability values of $P \leq 0.05$ were considered to be significant.

To identify differentially expressed genes between virus-associated CD8+ T-cells and nonassociated T-cells in human blood and plaque, the FindMarkers function in Seurat was used, calculating differential gene expressing using a nonparametric Wilcoxon rank-sum. Bonferroni-corrected *P* values were calculated based on the total number of genes in the dataset. Differential gene expression was visualized in a Volcano plot, using the EnhancedVolcano package.

RESULTS

Virus-Associated CD8+ T-Cells Accumulate in Human Atherosclerotic Lesions

To determine the number of virus-associated T-cells, T-cell receptor beta (TCRβ) sequencing was performed on 11 carotid endarterectomy samples and matched blood samples. The retrieved complementarity-determining region 3 sequences—the most variable region of the TCR, and essential for epitope binding—were compared with complementarity-determining region 3 sequences that were previously associated with virus infections, including IAV, EBV, and cytomegalovirus obtained from VDJdb,[29] mcPAS,[30] and TBAdb[31] databases. TCR sequencing resulted in 107 661 TCRβ templates in the blood, and 9993 TCRβ templates plaque, of which 1.08% and 1.84%, respectively appeared to be virus-associated. The percentage of virus-associated TCRβ sequences was significantly increased in the plaque samples, compared with patient-matched blood samples (Figure 1A; P=0.014), confirming previous reports that virus-specific CD8+ T-cells accumulate in the atherosclerotic lesion.[25,26] To explore whether virus-associated CD8+ T-cells accumulate because of a chronic inflammatory response or whether this phenomenon is particular to atherosclerosis, we evaluated the proportion of virus-associated CD8+ T-cells at another site of chronic inflammation. A previously published dataset containing TCRβ sequences from synovial fluid and patient-matched blood samples from psoriatic arthritis patients was utilized to evaluate the ratio of virus-associated TCRβ sequences between circulation and the site of inflammation.[33] Interestingly, virus-associated T-cells did not specifically home toward the inflamed synovium, indicating that virus-associated CD8+ T-cells do not accumulate at every site of chronic inflammation (Figure S2).

Virus-Associated CD8+ T-Cells Are More Clonally Expanded and Tissue Enriched Compared With Nonassociated CD8+ T-Cells

We next addressed whether virus-associated CD8+ T-cells differed in terms of T-cell clonality from nonvirus-associated CD8+ T-cells in the plaque, by evaluating the occurrence of each TCRβ sequence. We observed a significantly larger fraction of virus-associated clones that occurred at least more than once (expanded) compared with virus nonspecific clones, which more frequently showed single occurrences (Figure 1B; Figure S1A and S1C). To understand whether the expanded CD8+ T-cell clones specifically accumulated in the lesion, we next quantified their frequency in plaque compared with their frequency in PBMC. To address this question, CD8+ T-cell tissue-enrichment scores were determined by evaluating how frequently certain TCRβ sequences occurred in the plaque, compared with blood. TCRβ sequences were classified as plaque-enriched (higher occurrence in plaque compared with PBMCs), unenriched (same occurrence in plaque and PBMCs), plaque-single (only 1 occurrence in plaque, none in PBMCs), and PBMC-enriched (higher occurrence in PBMCs compared with plaque). Interestingly, no virus-associated TCRβ sequences in the lesion were PBMC-enriched. Moreover, virus-associated CD8+ T-cells trended toward a more plaque enrichment relative to other CD8+ T-cells in the lesion (Figure 1C; Figure S1B; P=0.08). This suggests that virus-associated CD8+ T-cells are specifically retained or locally expanded in the atherosclerotic plaque.

To investigate whether plaque enrichment of virus-associated CD8+ T-cells can be attributed to a single pathogen, we investigated whether IAV, EBV, cytomegalovirus, or other infectious agents contributed disproportionally to the number of expanded clones in the plaque in relation to blood (Figure 1D through 1H). In all blood samples and most plaque samples, T-cells associated with IAV, EBV, and cytomegalovirus could be detected, indicating that most donors have previously encountered these infections, confirmed by high seroconversion for cytomegalovirus in our patient population (65% seropositivity; Figure S4). However, we did not observe significant changes in the tissue distribution nor the contribution of each virus-associated CD8+ T-cell type to the total pool of expanded clones in blood or plaque.

Virus-Associated CD8+ T-Cells Show Signs of Recent TCR Activation in the Atherosclerotic Lesion

As TCRβ sequencing revealed that virus-associated CD8+ T-cells specifically accumulate in atherosclerotic lesions, we aimed to understand their activation pathways and potential role in the pathogenesis of atherosclerosis. To further interrogate the phenotype

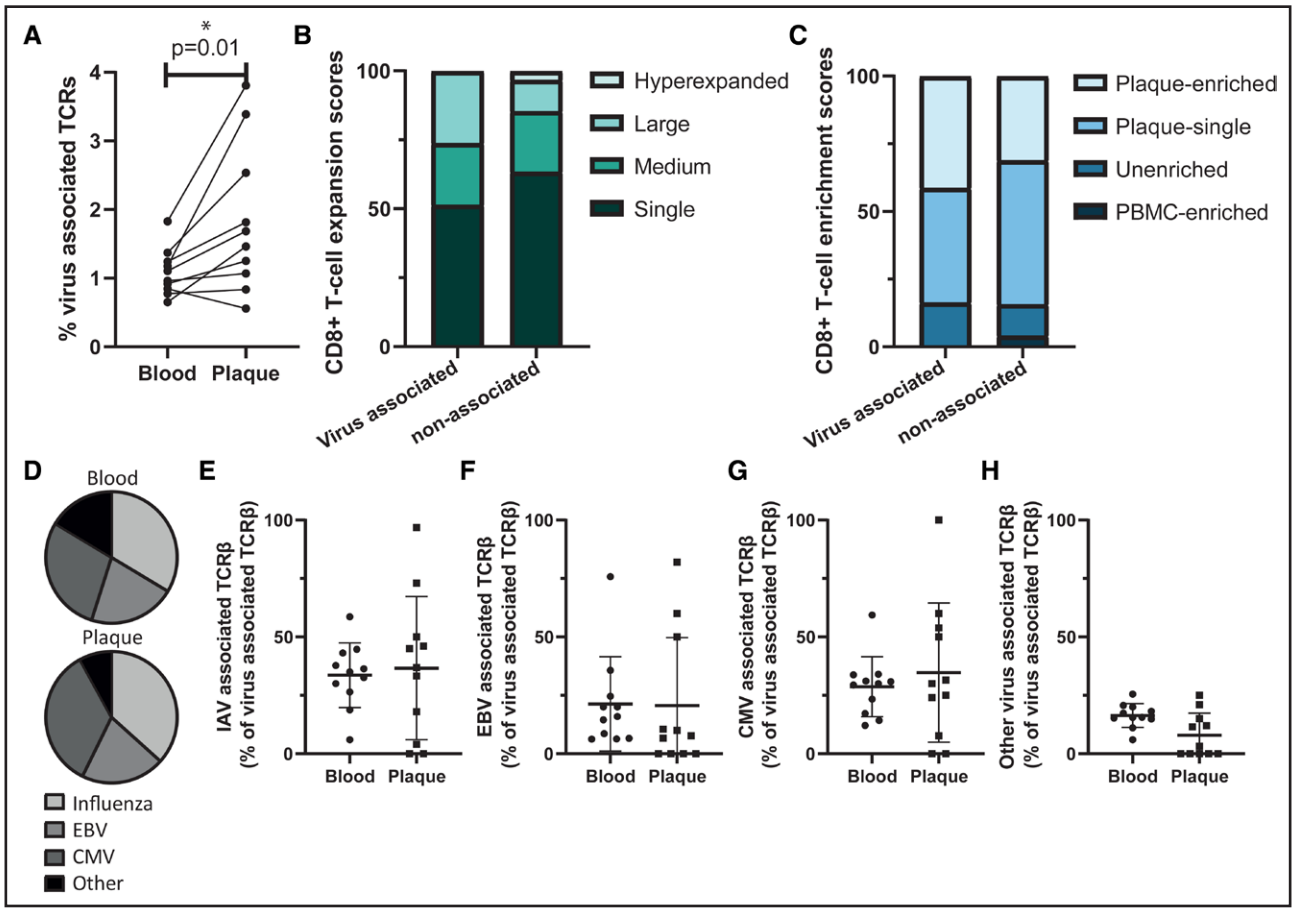

Figure 1. Virus-associated CD8+ T-cells accumulate in human atherosclerotic lesions.
A, Percentage of virus-associated CD8+ T-cells in human atherosclerotic lesions and patient-matched PBMC samples measured by matching T-cell receptor (TCR) sequences to TCR sequences of known specificity. **B**, Percentage of expanded CD8+ T-cells in the lesion. Expansion levels are divided into single (a single occurrence of a clonotype), medium (occurrence on >0.1 and ≤1% of all T-cells), large (occurrence on >1 and ≤10% of all T-cells), and hyper (occurrence on >10% of all T-cells). **C**, Percentage of enriched CD8+ T-cells in the lesion. Enrichment scores are divided into plaque-enriched (higher occurrence in plaque compared with PBMCs), plaque-single (single occurrence in plaque), unenriched (same occurrence in plaque and PBMCs), and PBMC enriched (higher occurrence in PBMCs compared with plaque). **D**, Pie charts representing the fractions of influenza (influenza A virus [IAV]), Epstein-Barr virus (EBV), CMV and other virus-associated CD8+ T-cells in blood (upper chart) and plaque (lower chart). Percentage of (**E**) IAV, (**F**) EBV, (**G**) CMV, and (**H**) other virus-associated CD8+ T-cells as a fraction of all virus-associated CD8+ T-cells in the human atherosclerotic lesion. Graphs present individual data points of (**A**) N=10, (**B** and **C**) N=9, or (**D** through **H**) N=11 patients, with mean±SD. Significance was determined by using a 2-tailed ratio pared Student *t* test (**A**), or a 2-way ANOVA with Bonferroni multiple comparisons (**E** through **H**), **P*<0.05, ***P*<0.001. CMV indicates cytomegalovirus; and PBMC, peripheral blood mononuclear cells.

of the virus-associated CD8+ T-cells in the atherosclerotic lesion, we used a scTCR-seq dataset of 3 human carotid endarterectomy samples and patient-matched blood samples, providing information on the TCRα and TCRβ sequence, and the transcriptome of the associated cells.[28] CD8+ T-cells were selected from this dataset based on featured barcoding for CD3 and CD8 and absence of CD4 and CD14 and subclustered. The CD8+ T-cell subclustering resulted in 9 conventional CD8+ T-cell clusters, including a naive CD8+ T-cell cluster (cluster 6), effector CD8+ T-cell clusters (cluster 0, 3, 5, and 10), a memory CD8+ T-cell cluster (cluster 2) and Temra clusters (cluster 1, 4, and 7; Figure 2A).[28] Virus-associated CD8+ T-cells were selected based on their TCRα or TCRβ sequence and projected to the various blood and plaque derived clusters (Figure 2B; Figure S5).

Virus-associated CD8+ T-cells showed a clear overrepresentation in the effector clusters in blood and plaque compared with the naive cluster. To evaluate phenotypic changes in situ, virus-associated CD8+ T-cells from blood were compared with their counterparts in the atherosclerotic lesion (Figure 2C). The transition from the blood toward the proinflammatory environment of the lesion results in the downregulation of genes associated with tissue egress,[37] apparent from a reduced expression of *S1PR1,* and *KLF2* in virus-associated CD8+ T-cells in the atherosclerotic lesion (Figure 2C and 2E). Interestingly, virus-associated CD8+ T-cells in the lesion also had a more activated phenotype, based

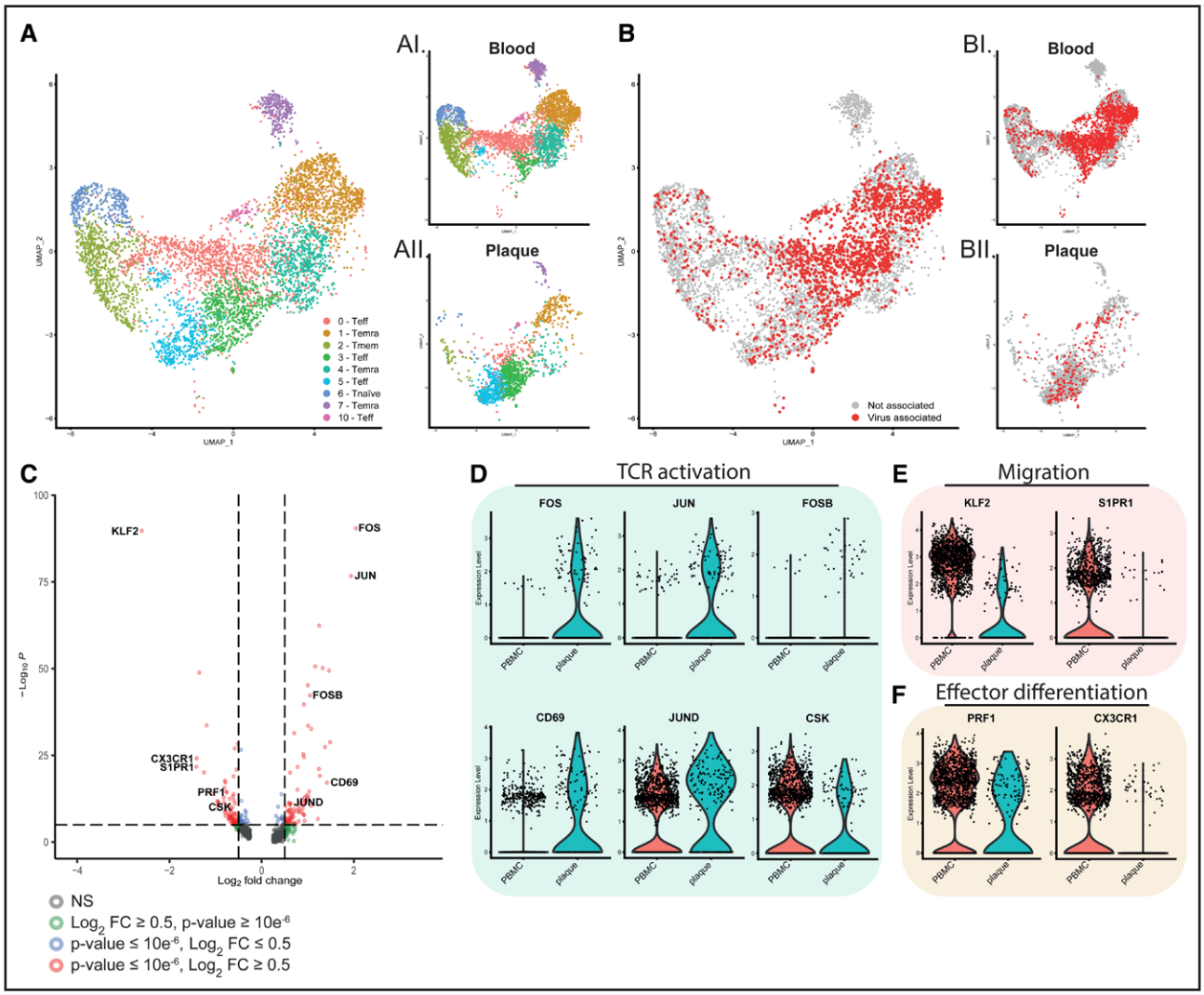

Figure 2. Virus-associated CD8+ T-cells in the lesion have a more activated phenotype compared with virus-associated CD8+ T-cells from blood.

A, UMAP visualization of unsupervised CD8+ T-cell clustering of single-cell T-cell receptor (TCR) sequencing analysis by Depuydt et al in human atherosclerotic lesions and patient-matched blood samples (number of cells=5730), (**AI**) split in blood originating CD8+ T-cells, (**AII**) and plaque-derived CD8+ T-cells. **B**, Projection of virus-associated CD8+ T-cells on unsupervised CD8+ T-cell clustering, based on TCRα and TCRβ sequences. **BI**, Projection of virus-associated CD8+ T-cells on blood clustering. **BII**, Projection of virus-associated CD8+ T-cells on plaque clustering. **C**, Volcano plot with differentially expressed genes between virus-associated CD8+ T-cells from plaque, compared with blood (left side, higher expression in blood; right side, higher expression in plaque). Genes were considered significant with a $P<10\times10^{-6}$ and a fold change of 0.5. Gene expression levels of significantly differentially expressed genes involved in (**D**) T-cell activation, (**E**) migration, and (**F**) effector differentiation, represented as violin plots. Analysis were performed on n=3 patients. FC indicates fold change; NS, not significant; and UMAP, uniform manifold approximation and projection.

on the increased expression of genes associated with TCR stimulation, including *FOS, JUN, FOSB, CD69,* and *JUND* and decreased expression of *CSK* (Figure 2C and 2D). These phenotypic changes are especially intriguing considering they are hallmarks for recent TCR activation,[38] hinting at in situ activation of virus-associated CD8+ T-cells. Aside from their more activated phenotype, these virus-associated CD8+ T-cells do not seem to become more cytotoxic in the atherosclerotic lesion, as genes involved in terminal effector differentiation, including *CX3CR1* and *PFR1*, were downregulated (Figure 2C and 2F).

Virus-Associated CD8+ T-Cells Are Phenotypically Highly Similar to Nonassociated CD8+ T-Cells in the s

To study how the activated phenotype of virus-associated CD8+ T-cells in the plaque relates to that of nonassociated CD8+ T-cells in the lesion, their transcriptomes were compared. Virus-associated CD8+ T-cells were evenly distributed over the different clusters in the lesion, as there are barely any naive T-cells present in the atherosclerotic lesion (Figure 3A and 3B). Only TemRA cluster 7 did not contain any virus-associated CD8+ T-cells. In line

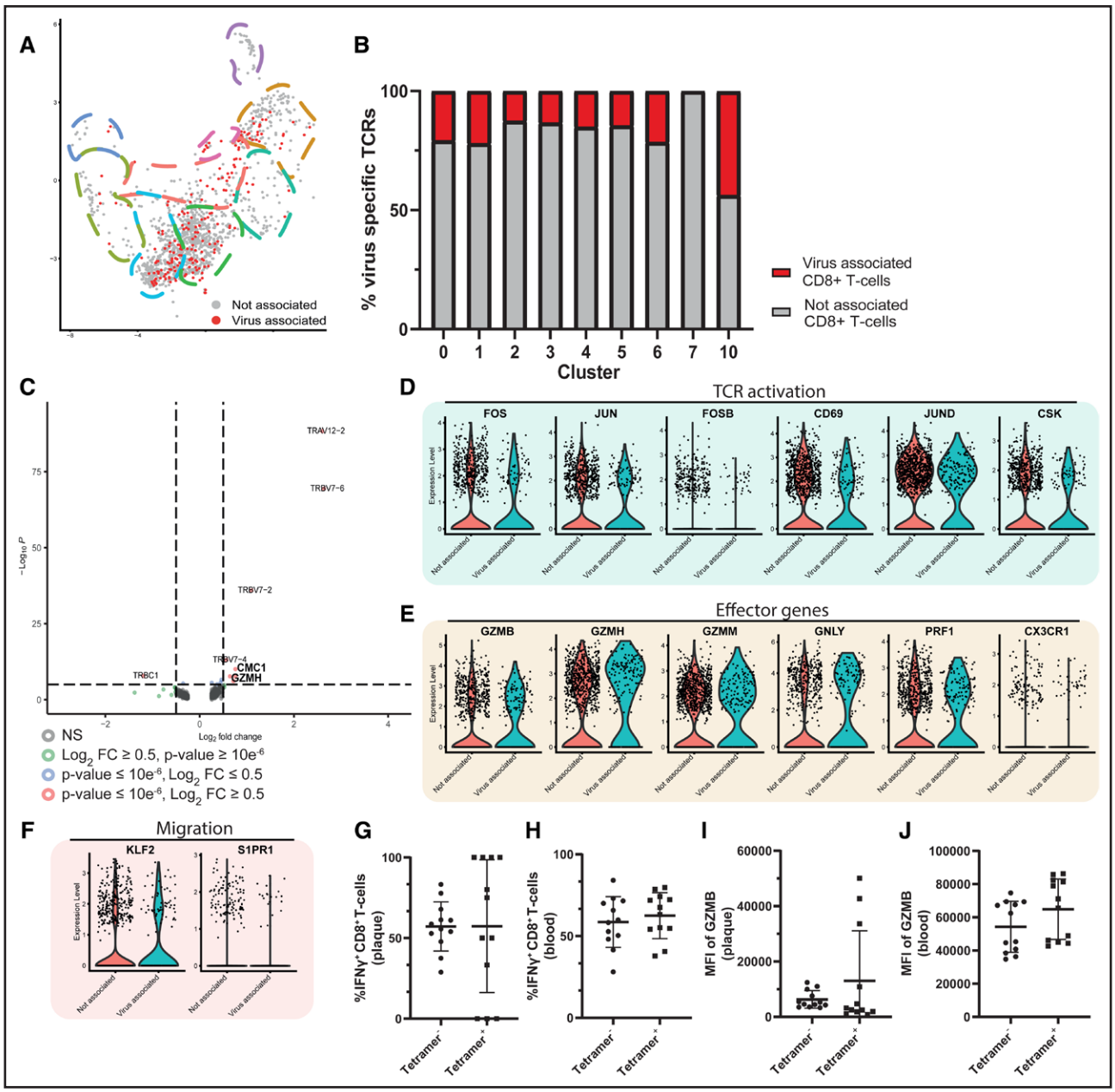

Figure 3. Virus-associated CD8+ T-cells are phenotypically and translationally highly similar to nonassociated CD8+ T-cells in the atherosclerotic lesion.

A, Projection of virus-associated CD8+ T-cells on unsupervised CD8+ T-cell clustering, visualizing virus-associated CD8+ T-cells per cluster. **B**, Percentage of virus-associated CD8+ T-cells per cluster in the plaque. **C**, Volcano plot with differentially expressed genes between virus-associated CD8+ T-cells, compared with nonassociated CD8+ T-cells from the lesion. Genes were considered significant with a $P<10\times10^{-6}$ and a fold change of 0.5. Expression levels of genes involved in (**D**) T-cell activation, (**E**) migration, and (**F**) effector differentiation, represented as violin plots. **G**, Percentage of IFNγ (interferon γ) expression by tetramer+ influenza A virus (IAV)/Epstein-Barr virus (EBV)-specific and tetramer- nonspecific CD8+ T-cells in the lesion, (**H**) and blood after 4 hours of stimulation with ionomycin and PMA (phorbol 12-myristate 13-acetate). **I**, MFI values of GZMB production by tetramer+ IAV/EBV-specific and tetramer- nonspecific CD8+ T-cells in the lesion, (**J**) and blood after stimulation. Analysis **A** through **F** were performed on N=3 patients. Graphs **G** and **H** present individual data points of N=12 patients, mean±SD. FC indicates fold change; MFI, mean fluorescence intensity; NS, not significant; and TCR, T-cell receptor.

with the uniform distribution of virus-associated CD8+ T-cells over the different clusters, phenotypic analysis revealed a high resemblance between virus-associated CD8+ T-cells and the nonassociated CD8+ T-cells in the lesion, with the only 2 differentially expressed genes being activation associated genes, *CMC1* and *GZMH* (Figure 3C). The protein encoded by *CMC1* is a component of the MITRAC (mitochondrial translation regulation assembly intermediate of cytochrome c oxidase) and is involved in the production of COX (cytochrome c oxidase), which is essential during T-cell activation. The *GZMH* gene, on the other hand, encodes the cytolytic

protein granzyme H. Beside *CMC1* and *GZMH*, expression level of other genes associated with T-cell activation or cytotoxicity remained unchanged between virus-associated CD8+ T-cells and nonassociated CD8+ T-cells in the atherosclerotic lesion (Figure 3D through 3F).

Virus-associated CD8+ T-cells were not only similar in phenotype to nonassociated CD8+ T-cells but also in cytotoxic potential, apparent from their comparable response to external stimuli. Single-cell suspensions of plaque and blood were stimulated for 4 hours with ionomycin and PMA to induce cytokine production. GILGFVTFL (IAV) or GLCTLVAML (EBV) specific CD8+ T-cells were detected using tetramers and cytokine and granzyme B production was assessed using flow cytometry. Indeed, IFNγ and granzyme B production of IAV- and EBV-specific CD8+ T-cells did not differ from cytokine production by nonassociated CD8+ T-cells in the lesion (Figure 3G and 3I; Figure S1). Interestingly, lesion-derived CD8+ T-cells expressed strongly reduced GZMB levels compared with CD8+ T-cells from circulation. This observation is in line with previous publication demonstrating that CD8+ T-cells from the atherosclerotic lesion exhibit a decreased inflammatory phenotype (Figure 3G through 3J).[39]

Virus-Derived Peptides Are Unlikely to Be Presented on HLA-I in Human Atherosclerotic Lesions

There are various ways by which CD8+ T-cells can be activated, including direct TCR activation or bystander activation.[40,41] To further explore whether virus-associated CD8+ T-cells can undergo TCR activation inside human atherosclerotic lesions, the immunopeptidome human atherosclerotic lesions was determined. Peptides expressed on HLA-I complexes in the lesion were eluted and sequenced using mass spectrometry and subsequently matched to the proteome of different pathogens, including IAV, EBV, and cytomegalovirus (Figure 4A).

Alignment of the lesion-derived HLA-I peptides with pathogenic proteomes revealed only 2 peptides, ATIQDIIRR and MAPRTLIL, which could originate from pathogens, but could also be derived from the human proteins endogenously expressed in the lesion (Figure S6). ATIQDIIRR is part of the highly conserved protein glycogen phosphorylase of *Chlamydia pneumoniae*, and cannot be distinguished by mass spectrometry from a human glycogen phosphorylase peptide (ATLQDIIRR). MAPRTLIL, on the other hand, is an amino acid sequence present in both the UL40 protein of cytomegalovirus and the human HLA-A protein. Although exogenous expression of *C. pneumonia*-derived ATIQDIIRR or cytomegalovirus-derived MAPRTLIL is possible, endogenous expression of the human counterparts seems more likely.

Immunopeptidomics Reveals a Potential Mimicry Response of Virus-Specific CD8+ T-Cells Against Autoantigens

As our data suggest it is highly unlikely that virus-specific CD8+ T-cells are directly triggered by virus-specific antigens in the plaque, we next investigated whether these T-cells may be activated through other TCR-specific mechanisms. A mechanism by which virus-associated CD8+ T-cells could exacerbate atherosclerosis in an antigen-specific manner, without local presentation of pathogen-derived peptides, is molecular mimicry. Mimicry peptides are foreign peptides that share a high homology in amino acid sequence and structure with self-antigens.

Although self-specific T-cells should be removed during positive selection in the thymus, there are numerous T-cell-mediated autoimmune disorders in which a role for molecular mimicry has been implicated, including multiple sclerosis, rheumatoid arthritis, Graves' disease, and diabetes.[42] Also, several articles focusing on the link between infectious diseases and cardiovascular disease already suggested a potential role of a mimicry response in cardiovascular disease.[26]

To investigate whether virus-associated T-cells might recognize self-peptides presented in the atherosclerotic lesions, we screened for self-peptides presented in the lesion with high homology (1 mismatch in amino acid sequence) to pathogen-derived peptides. This analysis resulted in a list of 85 mimicry peptides presented in the atherosclerotic lesion that were highly similar to pathogen-derived peptides (Figure 4B; Table S5). Approximately 10.6% of these peptides had a high homology with peptides derived from influenza, 5.9% matched peptides derived from cytomegalovirus, and 3.5% mimicked EBV-derived peptides (Figure 4C).

Aside from a high homology between a pathogen-derived peptide and a self-peptide, a molecular mimicry response against the atherosclerotic lesion can only be induced in case the mimicry peptide's master protein is exclusively expressed in the atherosclerotic lesion, and the pathogen-derived counterpart induces a sufficient CD8+ T-cell response during infection. However, most of the potential mimicry peptides presented in the lesion originated from proteins involved in general cellular processes, including cell migration, proliferation, and protein degradation, and are not specifically expressed in atherosclerotic lesions. Moreover, the capacity of the pathogen-derived peptides to induce a CD8+ T-cell response during infection was evaluated by predicting their binding affinity to the most frequently occurring HLA alleles, using the IEDB MHC-I-binding prediction tool.[43] Thirteen pathogen-derived peptides had a good predicted binding score (binding score >0.90) for at least one of the HLA alleles (Figure 4D; Table S6), but none of the peptides had a good binding prediction score for a wide range of HLA alleles. This means that a mimicry response against

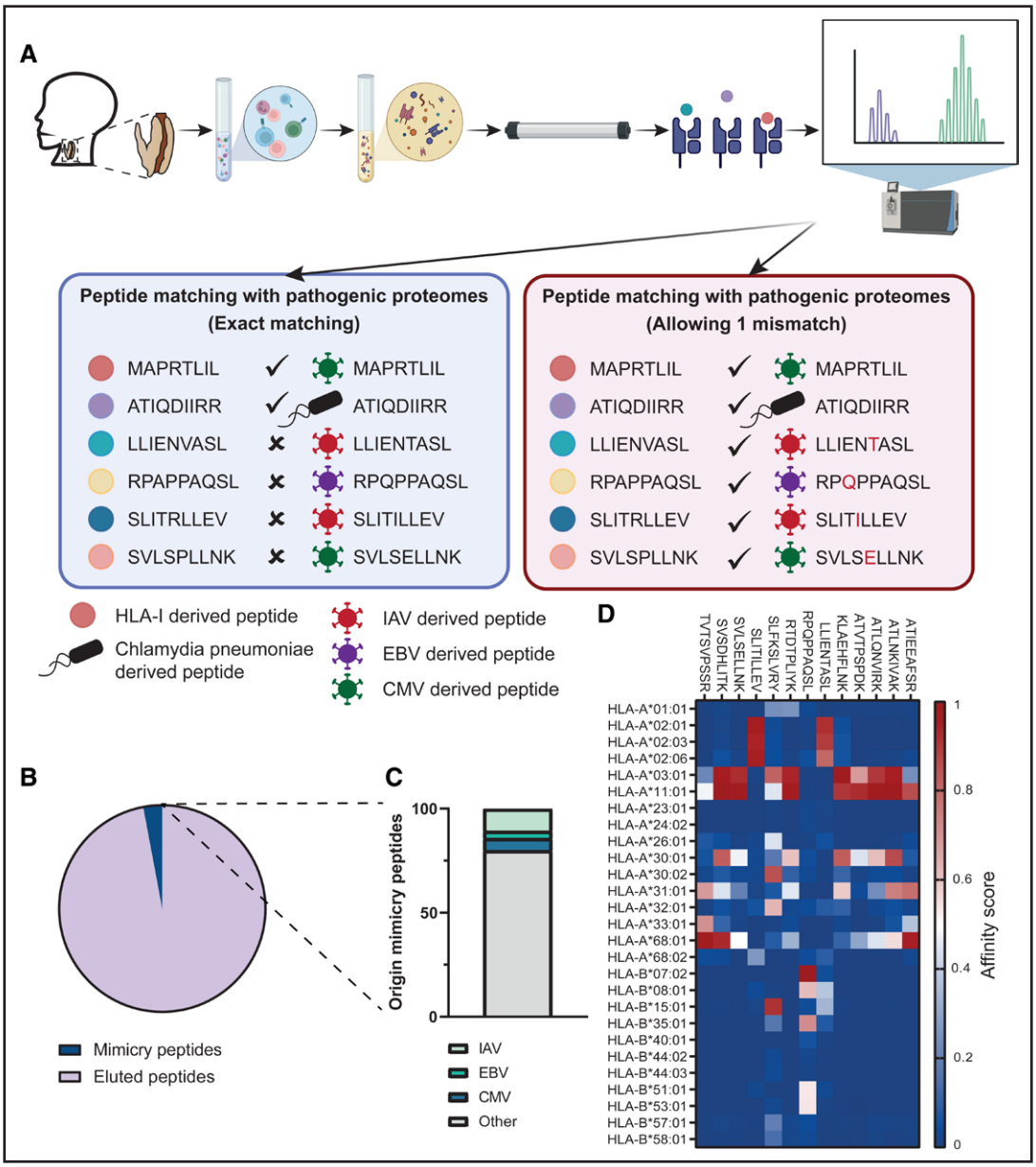

Figure 4. Virus-derived peptides are not presented on HLA-I in the atherosclerotic lesion.
A, Schematic overview of the experimental setup of immunopeptidomics analysis. Human endarterectomy samples were lysed, and HLA-I-peptide complexes were eluted by column containing pan HLA-I antibodies. Peptides were eluted from the HLA-I molecules and sequenced by mass spectrometry. Mass spectrometry results were matched with viral proteomes, identifying pathogen-derived peptides, or mimicry peptides presented in the lesion. **B**, Overview of peptides identified by immunopeptidomics, depicting the number of all eluted peptides and mimicry peptides (0.26%). **C**, Viral origin of mimicry peptides. **D**, Predicted binding scores of potential mimicry peptides to the most frequently occurring HLA types in the White population, predicted using IEDB. Predicted binding affinity is depicted in a colorimetric scale (blue=low-predicted binding affinity, red=good-predicted binding affinity). CMV indicates cytomegalovirus; EBV, Epstein-Barr virus; HLA, human leukocyte antigen; IAV, influenza A virus; PBMC, peripheral blood mononuclear cells; and TCR, T-cell receptor.

one of these peptides could only induce a response in a small fraction of the human population.

DISCUSSION

Virus infections have been associated with the progression of atherosclerosis since the early 20th century, and CD8+ T-cells targeting these infectious diseases have been detected inside human atherosclerotic lesions.[25,26] Our study demonstrates that virus-associated CD8+ T-cells accumulate in the lesion and are more clonally expanded and tissue enriched compared with nonassociated CD8+ T-cells, although these patients did not experience symptomatic infections at the time of surgery. We showed that at least 1.8% of the TCRs expressed in the atherosclerotic lesion were associated with viral

specificity, which is in line with previous findings.[26] This percentage was significantly higher compared with the percentage of virus-associated CD8+ T-cells in the blood, although the larger population of naive T-cells in the circulation may have diluted the percentage of virus-associated CD8+ T-cells in blood.

However, due to the increased clonality of virus-associated CD8+ T-cells in the atherosclerotic lesion, local expansion or retention of virus-associated CD8+ T-cells in the lesion seems probable. To investigate whether virus-associated CD8+ T-cells were locally expanded, we evaluated in situ activation of virus-specific CD8+ T-cells in the lesion using a single-cell TCR sequencing approach.[28] Plaque-residing virus-associated CD8+ T-cells expressed elevated levels of genes indicative of recent TCR engagement, including *CD69*, and AP-1 (activation protein-1) family members *FOS*, *FOSB*, *JUN*, and *JUND*.[44] Besides TCR engagement, an upregulated expression of both *CD69* and a variety of AP-1 family members has also been linked to a resident memory phenotype.[45] One might argue that the upregulation of these genes is simply a result of the transition from the circulation into the proinflammatory environment of the lesion, and is upregulated regardless of TCR stimulation.

The elevated expression of CD69 and AP-1 family members might indeed be the result of tissue infiltration, considering that all plaque-residing CD8+ T-cells exhibit heightened expression levels of these genes. Additionally, virus-associated CD8+ T-cells from the lesion were transcriptionally highly similar to other CD8+ T-cells located there and showed no signs of increased activation, migration, or cytotoxicity. Moreover, the virus-associated CD8+ T-cells distributed evenly over most CD8+ T-cell clusters, demonstrating they can obtain a variety of phenotypes in the atherosclerotic lesion. Interestingly, virus-associated CD8+ T-cells did not cluster together with cells from cytotoxic TemRA cluster 7, suggesting this cluster of terminally differentiated effector T-cells contains cells with specifies of nonviral origin.

One limitation of our approach is that we were only able to perform phenotypic characterization of virus-associated CD8+ T-cells in 3 patients. To strengthen the hypothesis that virus-associated CD8+ T-cells behave similarly to other T-cells residing in the lesion, we demonstrated comparable cytokine production and cytotoxic capacity of virus-associated CD8+ T-cells and nonassociated CD8+ T-cells from the atherosclerotic lesion in response to external stimuli in a larger cohort.

The similarity in phenotype between virus-associated CD8+ T-cells and nonassociated CD8+ T-cells in the lesion may be attributed to the absence of virus-derived antigens in the atherosclerotic plaque at the time of surgery. Sequencing of HLA-I-derived peptides from human plaques revealed only 2 potential pathogen-derived peptides: MAPRTLIL and ATIQDIIRR, which are associated with cytomegalovirus and *C. pneumoniae*, respectively. Although both cytomegalovirus and *C. pneumoniae* have been detected inside human atherosclerotic lesions,[46–48] it seems unlikely that these peptides are of pathogenic origin, as both peptides are indistinguishable from endogenous peptides by mass spectrometry. The MAPRTLIL amino acid sequence is also part of the human HLA-A protein, a protein highly expressed in human atherosclerotic lesions. ATIQDIIRR, on the other hand, could not be distinguished from a human glycogen phosphorylase peptide: ATLQDIIRR. Although ATLQDIIRR is only moderately expressed in the atherosclerotic lesion, multiple other peptides derived from glycogen phosphorylase were also presented on HLA-I (data not shown), making the endogenous expression of ATLQDIIRR highly likely.

In the absence of cognate antigens, CD8+ T-cells may be activated through cross-reactive mimicry peptides.[40] Chowdhury et al[26] postulated an atherosclerosis-specific mimicry response against TSPAN17 and ZIP9, 2 proteins highly expressed by endothelial cells, smooth muscle cells, and fibroblasts. They showed that influenza-specific TCRα and β sequence CASSIGLYGYTF-CAMSGGAGGTSYGKLTF (specific to the immunodominant peptide GILGFVFTL) was cross-reactive to epitopes derived from TSPAN17 and ZIP9. Despite the presence of endothelial cells, smooth muscle cells, and fibroblasts in our immunopeptidomics sample, we were not able to identify peptides derived from TSPAN17 or ZIP9, nor other proteins uniquely expressed in the plaque, which were expressed on HLA-I in the atherosclerotic lesion. Mimicry-induced cross-reactive T-cells are often directed against peptides specifically presented in the affected tissue; for example, mimicry-induced T-cell responses against insulin-derived peptides in diabetes.[49,50] Yet, the 85 potential mimicry peptides identified in this study originate from proteins involved in general cellular processes and are expressed in a wide variety of tissues. However, cross-reactivity can also be directed against tissue-specific posttranslational modification of proteins; for instance, the adverse reaction of T-cells against citrullinated proteins in rheumatoid arthritis.[51] In the atherosclerotic lesion, proteins can be posttranslationally modified via oxidation, acetylation, phosphorylation, succinylation, O-GlcNAcylation, methylation, ubiquitination, Sumoylation, glutathionylation, tyrosine nitration, and propionylation.[52] Only 2 out of 85 potential mimicry peptides presented posttranslational oxidation on methionine (Table S7), indicating that cross-reactivity of virus-associated CD8+ T-cells against posttranslationally modified mimicry peptides in the lesion is unlikely.

Based on this research it seems unlikely that virus-associated CD8+ T-cells are activated in an antigen-dependent manner in the absence of virus-derived antigen presentation. Nonetheless, these T-cells can induce an antigen-specific T-cell response during flare-ups of latent infections. Cytomegalovirus and EBV are

notorious for long-term latent infections, and respectively 33.7%[53] and 80%[54] of the carotid endarterectomy specimens show signs of latent infections.

In conclusion, virus-associated CD8+ T-cells are enriched in atherosclerotic lesions and are highly similar on a transcriptional level, to other plaque-residing CD8+ T-cells. The absence of virus-derived antigen presentation in the atherosclerotic lesion of patients without a symptomatic virus infection suggests that if these CD8+ T-cells contribute to inflammation, they probably do so through antigen-independent activation, or through a yet-to-be-identified mimicry response.

ARTICLE INFORMATION

Received December 7, 2023; accepted March 6, 2024.

Affiliations

Leiden Academic Centre for Drug Research, Division of BioTherapeutics, Leiden University, the Netherlands (M.J.M.J., F.H.S., M.A.C.D., F.L.V., J.K., I.B., B.S.). Department of Immunology, Leiden University Medical Centre, Center for Proteomics and Metabolomics, the Netherlands (G.M.C.J., P.v.V.). Department of Surgery, Haaglanden Medical Center – location Westeinde, Lijnbaan, The Hague, the Netherlands (J.A.H.M.P., L.G., A.W., H.J.S.).

Acknowledgments

Figure 4 was created with www.BioRender.com.

Sources of Funding

This work was supported by The Dutch Heart Foundation (CVON2017-20: GENIUS II, awarded to J. Kuiper), European Research Area Network on Cardiovascular Diseases (ERA-CVD, 2018T092, awarded to B. Slütter), the Dutch Heart Foundation (2019T067, awarded to I. Bot), and the Dutch Research Council (NWO) and ZonMw (Medium Investment Grant 91116004, awarded to P. van Veelen).

Disclosures

None.

Supplemental Material

Figures S1–S6
Tables S1–S8

REFERENCES

1. Kytömaa S, Hegde S, Claggett B, Udell JA, Rosamond W, Temte J, Nichol K, Wright JD, Solomon SD, Vardeny O. Association of influenza-like illness activity with hospitalizations for heart failure: the atherosclerosis risk in communities study. *JAMA Cardiol*. 2019;4:363–369. doi: 10.1001/jamacardio.2019.0549
2. Lanska DJ, Hoffmann RG. Seasonal variation in stroke mortality rates. *Neurology*. 1999;52:984–990. doi: 10.1212/wnl.52.5.984
3. Elkind MSV, Boehme AK, Smith CJ, Meisel A, Buckwalter MS. Infection as a stroke risk factor and determinant of outcome after stroke. *Stroke*. 2020;51:3156–3168. doi: 10.1161/STROKEAHA.120.030429
4. Kulick ER, Canning M, Parikh NS, Elkind MSV, Boehme AK. Seasonality of influenza-like-illness and acute cardiovascular events are related regardless of vaccine effectiveness. *J Am Heart Assoc*. 2020;9:16213. doi: 10.1161/JAHA.120.016213
5. Raisi-Estabragh Z, Cooper J, Salih A, Raman B, Lee AM, Neubauer S, Harvey NC, Petersen SE. Cardiovascular disease and mortality sequelae of COVID-19 in the UK Biobank Cardiac risk factors and prevention. *Heart*. 2022;109:1–8. doi: 10.1136/heartjnl-2022-321492
6. Behrouzi B, Bhatt DL, Cannon CP, Vardeny O, Lee DS, Solomon SD, Udell JA. Association of influenza vaccination with cardiovascular risk: a meta-analysis. *JAMA Netw Open*. 2022;5:e228873. doi: 10.1001/jamanetworkopen.2022.8873
7. Holodinsky JK, Zerna C, Malo S, Svenson LW, Hill MD. Association between influenza vaccination and risk of stroke in Alberta, Canada: a population-based study. *Lancet Public Health*. 2022;7:e914–e922. doi: 10.1016/S2468-2667(22)00222-5
8. Kim YE, Huh K, Park YJ, Peck KR, Jung J. Association between vaccination and acute myocardial infarction and ischemic stroke after COVID-19 infection. *JAMA*. 2022;328:887–889. doi: 10.1001/jama.2022.12992
9. Ren S, Newby D, Li SC, Walkom E, Miller P, Hure A, Attia J. Effect of the adult pneumococcal polysaccharide vaccine on cardiovascular disease: a systematic review and meta-analysis. *Open Heart*. 2015;2:e000247. doi: 10.1136/openhrt-2015-000247
10. Osler W. Diseases of the arteries. *Modern Med*. Philadelphia: Lea and Febiger; 1908.
11. Klotz O, Manning MF. Fatty streaks in the intima of arteries. *J Pathol Bacteriol*. 1911;16:211–220. doi: 10.1002/path.1700160117
12. Fabricant CG, Fabricant J, Litrenta MM, Minick CR. Virus-induced atherosclerosis. *J Exp Med*. 1978;148:335–340. doi: 10.1084/jem.148.1.335
13. Honarmand H. Atherosclerosis induced by *Chlamydophila pneumoniae*: a controversial theory. *Interdiscip Perspect Infect Dis*. 2013;2013:941392. doi: 10.1155/2013/941392
14. Behrouzi B, Udell JA. Moving the needle on atherosclerotic cardiovascular disease and heart failure with influenza vaccination. *Curr Atheroscler Rep*. 2021;23:1–10. doi: 10.1007/s11883-021-00973-w
15. Grzegorowska O, Lorkowski J. Possible correlations between atherosclerosis, acute coronary syndromes and COVID-19. *J Clin Med*. 2020;9:3746–3716. doi: 10.3390/jcm9113746
16. Khan S, Rahman HNA, Okamoto T, Matsunaga T, Fujiwara Y, Sawa T, Yoshitake J, Ono K, Ahmed KA, Rahaman MM, et al. Promotion of atherosclerosis by Helicobacter cinaedi infection that involves macrophage-driven pro-inflammatory responses. *Sci Rep*. 2014;4:1–12. doi: 10.1038/srep04680
17. Lee M, Baek H, Park JS, Kim S, Kyung C, Baik SJ, Lee BK, Kim JH, Ahn CW, Kim KR, et al. Current *Helicobacter pylori* infection is significantly associated with subclinical coronary atherosclerosis in healthy subjects: a cross-sectional study. *PLoS One*. 2018;13:e0193646. doi: 10.1371/journal.pone.0193646
18. Cristescu CV, Alain S, Ruță SM. The role of CMV infection in primary lesions, development and clinical expression of atherosclerosis. *J Clin Med*. 2022;11:3832. doi: 10.3390/jcm11133832
19. Wu YP, Sun DD, Wang Y, Liu W, Yang J. Herpes simplex virus type 1 and type 2 infection increases atherosclerosis risk: evidence based on a meta-analysis. *Biomed Res Int*. 2016;2016:2630865. doi: 10.1155/2016/2630865
20. Binkley PF, Cooke GE, Lesinski A, Taylor M, Chen M, Laskowski B, Waldman WJ, Ariza ME, Williams MV, Knight DA, et al. Evidence for the role of epstein barr virus infections in the pathogenesis of acute coronary events. *PLoS One*. 2013;8:e54008. doi: 10.1371/journal.pone.0054008
21. Campbell LA, Rosenfeld ME. Infection and atherosclerosis development. *Arch Med Res*. 2015;46:339–350. doi: 10.1016/j.arcmed.2015.05.006
22. Rosenfeld ME, Campbell LA. Pathogens and atherosclerosis: update on the potential contribution of multiple infectious organisms to the pathogenesis of atherosclerosis. *Thromb Haemost*. 2011;106:858–867. doi: 10.1160/TH11-06-0392
23. Gurevich VS, Pleskov VM, Levaya MV. Autoimmune nature of influenza atherogenicity. *Ann N Y Acad Sci*. 2005;1050:410–416. doi: 10.1196/annals.1313.092
24. Martínez-Salazar B, Holwerda M, Stüdle C, Piragyte I, Mercader N, Engelhardt B, Rieben R, Döring Y. COVID-19 and the vasculature: current aspects and long-term consequences. *Front Cell Dev Biol*. 2022;10:824851. doi: 10.3389/fcell.2022.824851
25. Keller TT, Van Der Meer JJ, Teeling P, Van Der Sluijs K, Idu MM, Rimmelzwaan GF, Levi M, Van Der Wal AC, De Boer OJ. Selective expansion of influenza A virus-specific T cells in symptomatic human carotid artery atherosclerotic plaques. *Stroke*. 2008;39:174–179. doi: 10.1161/STROKEAHA.107.491282
26. Chowdhury RR, D'Addabbo J, Huang X, Veizades S, Sasagawa K, Louis DM, Cheng P, Sokol J, Jensen A, Tso A, et al. Human coronary plaque T cells are clonal and cross-react to virus and self. *Circ Res*. 2022;130:1510–1530. doi: 10.1161/CIRCRESAHA.121.320090
27. Perez-Riverol Y, Bai J, Bandla C, García-Seisdedos D, Hewapathirana S, Kamatchinathan S, Kundu DJ, Prakash A, Frericks-Zipper A, Eisenacher M, et al. The PRIDE database resources in 2022: a hub for mass spectrometry-based proteomics evidences. *Nucleic Acids Res*. 2022;50:D543–D552. doi: 10.1093/nar/gkab1038
28. Depuydt MAC, Schaftenaar FH, Prange KHM, Boltjes A, Hemme E, Delfos L, De Mol J, De Jong MJM, Kleijn MNAB, Peeters JAHM, et al. Single-cell T cell receptor sequencing of paired human atherosclerotic plaques and blood reveals autoimmune-like features of expanded effector T cells. *Nat Cardiovasc Res*. 2023;2:1–14. doi: 10.1038/s44161-022-00208-4

29. Shugay M, Bagaev DV, Zvyagin IV, Vroomans RM, Crawford JC, Dolton G, Komech EA, Sycheva AL, Koneva AE, Egorov ES, et al. VDJdb: a curated database of T-cell receptor sequences with known antigen specificity. *Nucleic Acids Res*. 2018;46:D419–D427. doi: 10.1093/nar/gkx760
30. Tickotsky N, Sagiv T, Prilusky J, Shifrut E, Friedman N. McPAS-TCR: a manually curated catalogue of pathology-associated T cell receptor sequences. *Bioinformatics*. 2017;33:2924–2929. doi: 10.1093/bioinformatics/btx286
31. Chen SY, Yue T, Lei Q, Guo AY. TCRdb: a comprehensive database for T-cell receptor sequences with powerful search function. *Nucleic Acids Res*. 2021;49:D468–D474. doi: 10.1093/nar/gkaa796
32. Wickham H, Averick M, Bryan J, Chang W, D' L, Mcgowan A, François R, Grolemund G, Hayes A, Henry L, et al. Welcome to the tidyverse. *J Open Source Softw*. 2019;4:1686. doi: 10.21105/joss.01686
33. Komech EA, Koltakova AD, Barinova AA, Minervina AA, Salnikova MA, Shmidt EI, Korotaeva TV, Loginova EY, Erdes SF, Bogdanova EA, et al. TCR repertoire profiling revealed antigen-driven CD8+ T cell clonal groups shared in synovial fluid of patients with spondyloarthritis. *Front Immunol*. 2022;13:973243. doi: 10.3389/fimmu.2022.973243
34. Blighe K, Rana S, Lewis M. EnhancedVolcano: Publication-ready volcano plots with enhanced colouring and labeling. 2018.
35. Hassan C, Kester MGD, de Ru AH, Hombrink P, Drijfhout JW, Nijveen H, Leunissen JAM, Heemskerk MHM, Falkenburg JHF, van Veelen PA. The human leukocyte antigen–presented ligandome of B lymphocytes. *Mol Cell Proteomics*. 2013;12:1829–1843. doi: 10.1074/mcp.M112.024810
36. Manber U, Wu S. approximate GREP for fast fuzzy string searching. GitHub. https://github.com/Wikinaut/agrep
37. Yang X-X, Yang C, Wang L, Zhou Y-B, Yuan X, Xiang N, Wang Y-P, Li X-M. Molecular mechanism of sphingosine-1-phosphate receptor 1 regulating CD4 + tissue memory in situ T cells in primary Sjogren's syndrome. *Int J Gen Med*. 2021;14:6177–6188. doi: 10.2147/IJGM.S327304
38. Garces de Los Fayos Alonso I, Liang HC, Turner SD, Lagger S, Merkel O, Kenner L. The role of Activator Protein-1 (AP-1) family members in CD30-positive lymphomas. *Cancers (Basel)*. 2018;10:93. doi: 10.3390/cancers10040093
39. van Duijn J, van Elsas M, Benne N, Depuydt M, Wezel A, Smeets H, Bot I, Jiskoot W, Kuiper J, Slütter B. CD39 identifies a microenvironment-specific anti-inflammatory CD8 + T-cell population in atherosclerotic lesions. *Atherosclerosis*. 2019;285:71–78. doi: 10.1016/j.atherosclerosis.2019.04.217
40. Cusick MF, Libbey JE, Fujinami RS. Molecular mimicry as a mechanism of autoimmune disease. *Clin Rev Allergy Immunol*. 2012;42:102–111. doi: 10.1007/s12016-011-8294-7
41. Kim TS, Shin EC. The activation of bystander CD8+ T cells and their roles in viral infection. *Exp Mol Med*. 2019;51:1–9. doi: 10.1038/s12276-019-0316-1
42. Rojas M, Restrepo-Jiménez P, Monsalve DM, Pacheco Y, Acosta-Ampudia Y, Ramírez-Santana C, Leung PSC, Ansari AA, Gershwin ME, Anaya JM. Molecular mimicry and autoimmunity. *J Autoimmun*. 2018;95:100–123. doi: 10.1016/j.jaut.2018.10.012
43. HLA allele frequencies and reference sets with maximal population coverage – IEDB Solutions Center. https://help.iedb.org/hc/en-us/articles/114094151851
44. Hughes CC, Pober JS. Costimulation of peripheral blood T cell activation by human endothelial cells. Enhanced IL-2 transcription correlates with increased c-fos synthesis and increased Fos content of AP-1. *J Immunol*. 1993;150:3148–3160. doi: 10.4049/jimmunol.150.8.3148
45. Chen Y, Shen J, Kasmani MY, Topchyan P, Cui W. Single-cell transcriptomics reveals core regulatory programs that determine the heterogeneity of circulating and tissue-resident memory cd8+ t cells. *Cells*. 2021;10:2143. doi: 10.3390/cells10082143
46. Otani T, Nishihira K, Azuma Y, Yamashita A, Shibata Y, Asada Y, Hatakeyama K. *Chlamydia pneumoniae* is prevalent in symptomatic coronary atherosclerotic plaque samples obtained from directional coronary atherectomy, but its quantity is not associated with plaque instability: an immunohistochemical and molecular study. *Clin Pathol*. 2022;15:2632010X221125179. doi: 10.1177/2632010X221125179
47. Melnick JL, Hu C, Burek J, Adam E, Debakey ME. Cytomegalovirus DNA in arterial walls of patients with atherosclerosis. *J Med Virol*. 1994;42:170–174. doi: 10.1002/jmv.1890420213
48. Nerheim PL, Meier JL, Vasef MA, Li WG, Hu L, Rice JB, Gavrila D, Richenbacher WE, Weintraub NL. Enhanced cytomegalovirus infection in atherosclerotic human blood vessels. *Am J Pathol*. 2004;164:589–600. doi: 10.1016/S0002-9440(10)63148-3
49. Girdhar K, Huang Q, Chow IT, Vatanen T, Brady C, Raisingani A, Autissier P, Atkinson MA, Kwok WW, Ronald Kahn C, et al. A gut microbial peptide and molecular mimicry in the pathogenesis of type 1 diabetes. *Proc Natl Acad Sci USA*. 2022;119:e2120028119. doi: 10.1073/pnas.2120028119
50. García AR, Paterou A, Lee M, Sławiński H, Wicker LS, Todd JA, Pękalski ML. Peripheral tolerance to insulin is encoded by mimicry in the microbiome. *bioRxiv*. 2019;2019.12.18.881433. https://www.biorxiv.org/content/10.1101/2019.12.18.881433v1
51. Darrah E, Andrade F. Rheumatoid arthritis and citrullination. *Curr Opin Rheumatol*. 2018;30:72–78. doi: 10.1097/BOR.0000000000000452
52. Liu YP, Zhang TN, Wen R, Liu CF, Yang N. Role of posttranslational modifications of proteins in cardiovascular disease. *Oxid Med Cell Longev*. 2022;2022:3137329. doi: 10.1155/2022/3137329
53. Jia YJ, Liu J, Han FF, Wan ZR, Gong LL, Liu H, Zhang W, Wardell T, Lv YL, Liu LH. Cytomegalovirus infection and atherosclerosis risk: a meta-analysis. *J Med Virol*. 2017;89:2196–2206. doi: 10.1002/jmv.24858
54. De Boer OJ, Teeling P, Idu MM, Becker AE, van der Wal AC. Epstein Barr virus specific T-cells generated from unstable human atherosclerotic lesions: implications for plaque inflammation. *Atherosclerosis*. 2006;184:322–329. doi: 10.1016/j.atherosclerosis.2005.05.001